Desalination and Water Treatment
www.deswater.com

doi: 10.5004/dwt.2019.22989

137 (2019) 34–40
January

Research on dynamic synergistic scale inhibition performance and mechanisms of ESA/IA/AMPS copolymer with electrostatic field

Meifang Yan[a,b,c,d], Qiangqiang Tan[a,b,*], Haihua Li[c,d], Lihui Zhang[c,d], Zhenfa Liu[c,d,*]

[a]*State Key Laboratory of Multiphase Complex Systems, Institute of Process Engineering, Chinese Academy of Sciences, No. 19A Yuquan Road, Beijing, China, Tel. +86 1062529377; emails: qtan@ipe.ac.cn (Q. Tan), yanmeifang525@sina.com (M. Yan)*
[b]*University of Chinese Academy of Sciences, Beijing 100049, China*
[c]*Institute of Energy Resources, Hebei Academy of Science, No. 46 Youyi South Street Shijiazhuang, China, Tel. +86 31183031008; emails: lzf63@sohu.com (Z. Liu), c.t.0205@sina.com (H. Li), zlhkxy@sohu.com (L. Zhang)*
[d]*Hebei Engineering Research Center for Water Saving in Industry, Shijiazhuang 0500811, China*

Received 30 January 2018; Accepted 18 August 2018

ABSTRACT

Dynamic scale inhibition of epoxysuccinic acid/itaconic acid/2-acrylamido-2-methyl propanesulfonic acid (ESA/IA/AMPS) copolymer with electrostatic field was studied via a dynamic simulation device. $CaCO_3$ morphology and crystal form were characterized by scanning electron microscope (SEM) and X-ray diffraction (XRD). The results show an obvious synergistic effect between the electrostatic field and ESA/IA/AMPS copolymer in a dynamic scale inhibition test. The synergism scale inhibition rate was 95.85%, which is 12.94% higher when compared with the copolymer alone. SEM and XRD analyses indicate that the electrostatic field facilitated the formation of aragonite $CaCO_3$. $CaCO_3$ scale formation in a blank water sample consisted of 83.8% calcite and 16.2% aragonite, while $CaCO_3$ scale formation from a water sample treated with an electrostatic field consisted of 95.5% aragonite and 4.5% calcite. The $CaCO_3$ scale formed in the presence of the copolymer and formed under the synergistic effect both consisted of 100% aragonite. However, $CaCO_3$ crystal particles that formed under the synergistic effect were much smaller and more dispersed.

Keywords: Dynamic scale inhibition; ESA/IA/AMPS copolymer; Electrostatic field; Synergism; $CaCO_3$ crystal form

1. Introduction

Various mineral salts are found in water used in industrial circulating cooling water systems, especially calcium bicarbonate. Calcium bicarbonate is unstable and easily decomposes to carbonate. Carbonate is stable and easily adheres to the surface of heat exchangers, causing a decline in the heat conduction and influencing the heat transfer efficiency of the exchanger. Moreover, the heat exchanger cannot run normally. At present, the most effective method of inhibiting calcium carbonate scale formation is adding chemicals to the circulating water system. However, the addition of large amounts of chemicals has led to secondary pollution.

With the increase in human environmental awareness, recent water treatment research has been focused on green water treatment chemicals and clean technologies [1,2]. Physical water treatment methods, such as magnetism, ultrasound, and static electric field, offer advantages, such as ease of operation, low-cost maintenance, and nontoxicity, compared with chemical treatments. However, these methods have some limitations. Electrostatic water treatment was developed in recent decades as a type of physical water treatment technology, and it exhibits unique performance characteristics in water treatment [3–10]. Electrostatic water treatment technology is appealing because of its low-energy consumption (the power dissipation of an ESC-100

* Corresponding author.

1944-3994/1944-3986 © 2019 Desalination Publications. All rights reserved.

electrostatic water treatment device is 15 W) and ability to reduce pollution. However, it does not sufficiently inhibit $CaCO_3$ scale formation when used as the sole water treatment technique.

Polyepoxysuccinic acid (PESA) is a nonphosphorus, nonnitrogen water treatment agent with good degradation properties [11–13]. However, the scale inhibition against $CaCO_3$ formation is not sufficient when used in water with high hardness and alkalinity. PESA has little effect on $Ca_3(PO_4)_2$ inhibition and Fe_2O_3 dispersal. PESA derivatives are synthesized by introducing specific functional groups to enhance their performance [14–17]. ESA/IA/AMPS copolymer is one such derivative, in which sulfonic and carboxylic acid group are introduced into PESA [17]. In the application of the copolymer, the results showed that the scale inhibition rate was 80.9% against $CaCO_3$ and 100% against $Ca_3(PO_4)_2$ at a dosage of 30 mg/L ESA/IA/AMPS copolymer. The copolymer exhibited good dispersion and biodegradation properties, but the dosage was high. To reduce the dosage of the water treatment agent, electrostatic water treatment and ESA/IA/AMPS copolymer were combined in this paper. The synergistic scale inhibition of the copolymer with an electrostatic field and the effect on $CaCO_3$ crystal formation were studied.

2. Experimental

2.1. Chemicals and reagents

The chemicals used in this study included analytical grade calcium chloride dehydrate, sodium bicarbonate, and ethylenediamine tetraacetic acid. The water treatment agent ESA/IA/AMPS copolymer was synthesized using a previously published method [17].

2.2. Water samples

Underground water, which was collected from the residential subdistricts in the city of Shijiazhuang, was used to study synergistic scale inhibition. A simulated water sample containing 400 mg/L Ca^{2+} and 400 mg/L HCO_3^- (as $CaCO_3$) was made with analytical grade calcium chloride dehydrate and sodium bicarbonate, and this sample was used to study the crystal form of calcium carbonate.

2.3. Testing apparatus

2.3.1. Electrostatic water treatment device

As seen in Fig. 1, the electrostatic water treatment device consists of water treatment equipment (ϕ35 × 800 mm) and a high-voltage DC power supply. The electrostatic voltage range is 2–8 kV. The anode of the device is a conductive metal rod, and it is placed in a tetrafluoroethylene cylinder. The cathode is a seamless steel pipe. The anode and cathode are kept at a certain distance and form a cavity. The output of the high voltage power supply is connected to the metal rod of the water treatment equipment. The ground wire is connected to shell of the water treatment equipment. A high voltage electrostatic field is obtained by adjusting the power supply voltage, and the electrostatic field impacts the flow rate of the water in the cavity.

2.3.2. Dynamic simulation water treatment device

The electrostatic water treatment device was connected to a DGC-III dynamic simulation device in order to monitor electrode fouling. A schematic of the device is shown in Fig. 2.

The heat exchanger consisted of glass bushing and a stainless steel heat pipe. Water samples flowed into the space between the drive pipe and heat transfer pipe. Water samples in the water channel below flowed through the electrostatic water treatment device and into the water channel above. Next, water samples flowed through the heat exchanger, and scale adhered to the surface of the heat transfer pipe. This resulted in fouling resistance, which led to a decrease in the heat transfer coefficient of the heat exchanger as well as a decrease in heat transfer performance. The dynamic synergistic scale inhibition performance was evaluated by studying the changes in fouling resistance.

2.4. Evaluation of dynamic scale inhibition

Underground water was used in the dynamic scale inhibition experiments, and the composition of water samples was as follows: total hardness of 791 mg/L (as $CaCO_3$), Ca^{2+} hardness of 585 mg/L (as $CaCO_3$), total alkalinity of 317 mg/L (as $CaCO_3$), and Cl^- content of 244 mg/L.

Test conditions were as follows: the experiment temperature was 40°C, experiment time was 10 h, and heating

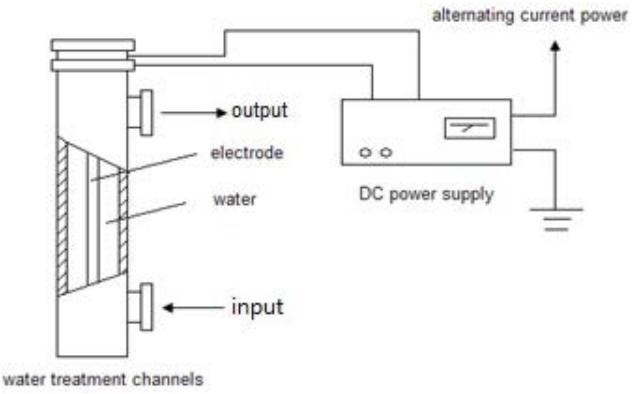

Fig. 1. Schematic of electrostatic water treatment system.

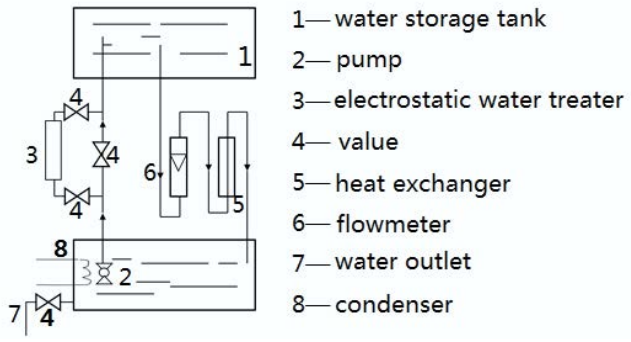

Fig. 2. Dynamic simulation of the electrostatic water treatment device.

voltage was 5 V. According to the heat transfer rate equation, the thermal resistance was calculated in Eq. (1) as follows:

$$R_d = \frac{A}{Q}\left(\Delta T_{md} - \Delta T_{mc}\right) \quad (1)$$

where R_d (m^2 K/W) is thermal resistance, A (m^2) is heat transfer area, Q (W) is heat transfer rate, ΔT_{md} (K) and ΔT_{mc} (K) are the average temperature difference between the water and the heat exchanger after and before scale formation, respectively.

The dynamic scale inhibition rate was calculated in Eq. (2) as follows:

$$\eta = \left(1 - \frac{R_{d'}}{R_d}\right) \times 100\% \quad (2)$$

where $R_{d'}$ (m^2 K/W) is the fouling resistance, with the water treatment agent or with both the agent and an electrostatic field and R_d (m^2 K/W) is the fouling resistance of a blank water sample.

2.5. Characterization of $CaCO_3$ scale samples

A water sample containing 400 mg/L Ca^{2+} and 400 mg/L HCO_3^- (as $CaCO_3$) was made with analytical grade calcium chloride dehydrate and sodium bicarbonate. Four $CaCO_3$ samples to be prepared: $CaCO_3$ sample from blank water, $CaCO_3$ sample from water treated with an electrostatic field, $CaCO_3$ sample from water treated with the ESA/IA/AMPS copolymer, and $CaCO_3$ sample from water treated with an electrostatic field and the copolymer. A glass slide was placed in the water storage tank before the dynamic inhibition scale experiment. The experimental conditions were as follows: temperature of 55°C, electrostatic voltage of 5 kV, flow rate of 80 L/h, and experiment time of 10 h. When the experiment was completed, the glass slide was removed and dried at 40°C. The glass slide was fixed to the sample table by conductive adhesive tape, and the morphology of $CaCO_3$ scale precipitate was observed by scanning electron microscope (SEM, Inspect S50, FEI). The accelerating voltage was 20 kV, and the magnification was 2,000.

The crystal texture of $CaCO_3$ was characterized by X-ray diffraction (XRD). The test conditions were as follows: Cu target, working voltage of 40 kV, scanning range of 20°–60°, step length of 0.02°, and scanning speed of 2°/s. Based on the adiabatic method of quantitative analysis, the mass fraction of every phase (W_X) was calculated in Eq. (3) as follows:

$$W_X = \frac{I_X}{\frac{RIR_X}{RIR_C} \times \sum_{i=C}^{N} \frac{I_i}{K_C^i}} = \frac{I_X}{K_C^X \sum_{i=C}^{N} \frac{I_i}{K_C^i}} \quad (3)$$

where I_X is the maximum diffraction peak area of X phase; RIR_C is the reference intensity of internal standard substance; and RIR_X is the reference intensity of X phase. K_c^i is the ratio of the diffraction peak area of i phase to the peak area of the internal standard.

3. Results and discussion

3.1. Dynamic synergistic scale inhibition of electrostatic field and ESA/IA/AMPS copolymer

3.1.1. Effect of ESA/IA/AMPS copolymer concentration on synergistic scale inhibition

The influence of ESA/IA/AMPS copolymer concentration on dynamic synergistic inhibition against $CaCO_3$ scale was studied using the following conditions: electrostatic voltage of 5 kV and flow rate of 80 L/h. The analysis of the water samples is described in Section 2.4. Fig. 3 shows the changes in fouling resistance overtime. Table 1 shows the fouling resistance of different copolymer concentrations and Table 2 shows the dynamic scale inhibition rate of different copolymer concentrations.

As the copolymer concentration increased, the fouling resistance decreased, and the scale inhibition rate was improved when using the agent alone or using the electrostatic field with the agent. The dynamic synergistic scale inhibition rate was higher than when the copolymer was used alone at any concentration in the experiment. When the concentration of the copolymer was 1.0 mg/L, the scale inhibition rate increased by 12.94%, which was the highest value achieved. This suggests that distinct synergistic scale inhibition exists

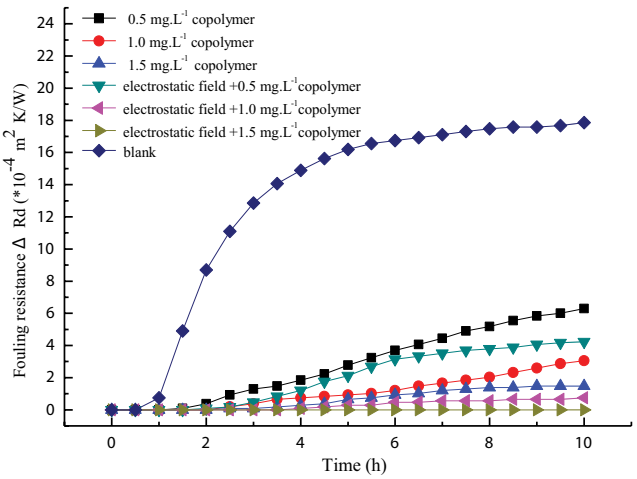

Fig. 3. The effects of different copolymer concentrations on dynamic fouling resistance.

Table 1
Dynamic fouling resistance of different copolymer concentrations

Concentration (mg/L)	Fouling resistance (×10⁻⁴ m² K/W)		
	Blank	Copolymer	Electrostatic field + copolymer
0.5	17.85	6.29	4.26
1.0		3.05	0.74
1.5		1.48	0

Operating conditions: electrostatic voltage of 5 kV, flow rate of 80 L/h, experiment temperature of 40°C, and experiment time of 10 h.

Table 2
Dynamic scale inhibition rate of different copolymer concentrations

Concentration (mg/L)	Scale inhibition rate (%)		Scale inhibition rate increment (%)
	Copolymer	Electrostatic field + copolymer	
0.5	64.76	76.13	11.37
1.0	82.91	95.85	12.94
1.5	91.71	100	8.29

Operating conditions: electrostatic voltage of 5 kV, flow rate of 80 L/h, experiment temperature of 40°C, and experiment time of 10 h.

between the electrostatic field and ESA/IA/AMPS copolymer. When the concentration of the copolymer was 1.5 mg/L, the scale inhibition rate was 91.71%, for the copolymer alone. The dynamic synergistic scale inhibition rate was 95.85% at a copolymer concentration of 1.0 mg/L. The concentration was reduced by one-third when using the synergistic treatment of electrostatic field with ESA/IA/AMPS copolymer, and almost the same scale inhibition effect was achieved.

3.1.2. The effect of electrostatic voltage on synergistic scale inhibition

For this section, the experimental conditions were as follows: flow rate of 80 L/h and a copolymer concentration of 1.0 mg/L. The analysis of the water samples is described in Section 2.4. Fig. 4 shows the changes in fouling resistance with different electrostatic voltages overtime. Table 3 shows the dynamic fouling resistance at different voltages and Table 4 shows the dynamic scale inhibition rate at different voltages.

With increasing electrostatic voltage, the fouling resistance decreased, and the scale inhibition rate increased when the copolymer and the electrostatic field were used

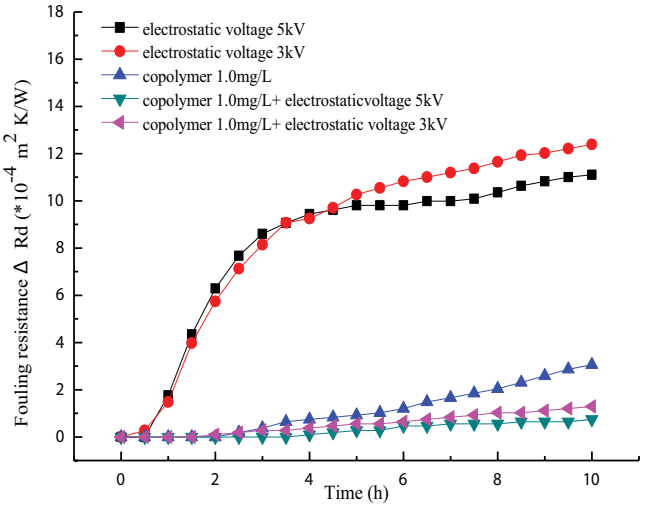

Fig. 4. The effect of electrostatic voltage on dynamic fouling resistance.

respectively or in combination. When the electrostatic field and the copolymer were used in combination, the increase in synergistic scale inhibition rate was greater than when the copolymer was used as the sole. When the static voltage was 3 kV, the inhibition rate was 9.81% higher for the combined than for the copolymer alone. When the static voltage was 5 kV, the increment of synergism scale inhibition rate was 12.94%, and the synergism scale inhibition rate was 95.85%.

3.2. Influence of synergism on the morphology and crystal form of $CaCO_3$

3.2.1. SEM analysis of $CaCO_3$

$CaCO_3$ scale samples were prepared according to the method and experimental conditions in Section 2.5.

Table 3
Dynamic fouling resistance at different voltages

Electrostatic voltage (kV)	Fouling resistance ($\times 10^{-4}$ m^2 K/W)			
	Blank	Electrostatic field	Electrostatic field + copolymer	Copolymer
3	17.85	12.40	1.30	3.05
5		11.10	0.74	

Operating conditions: flow rate of 80 L/h, copolymer concentration of 1.0 mg/L, experiment temperature of 40°C, and experiment time of 10 h.

Table 4
Dynamic scale inhibition rate at different voltages

Electrostatic voltage (kV)	Scale inhibition rate (%)			Scale inhibition rate increment (%)
	Electrostatic field	Electrostatic field + copolymer	Copolymer	
3	30.53	92.72	82.91	9.81
5	37.82	95.85		12.94

Operating conditions: flow rate of 80 L/h, copolymer concentration of 1.0 mg/L, experiment temperature of 40°C, and experiment time of 10 h.

As shown in Fig. 5, $CaCO_3$ crystals from the blank water sample were rhombohedron calcite and small amounts of needle-shaped aragonite. When the blank water was treated with an electrostatic field, the amount of needlelike aragonite $CaCO_3$ increased and the length of the aragonite particles decreased, and the amount of calcite $CaCO_3$ decreased (in Fig. 6). The $CaCO_3$ crystals from the blank water sample treated with the copolymer were completely transformed into needle-like aragonite (in Fig. 7), and the particles were densely packed. The synergism effect also transformed the $CaCO_3$ crystals into needle-like aragonite (in Fig. 8). Compared with Fig. 7, the crystals shown in Fig. 8 were more dispersed, the particles were smaller, and they did not easily adhere to the surface of the heat exchanger. As a result, the fouling resistance decreased, and the scale inhibition rate increased. The synergism enhanced the chelating properties of the inhibitor for calcium ions upon application of the static electric field.

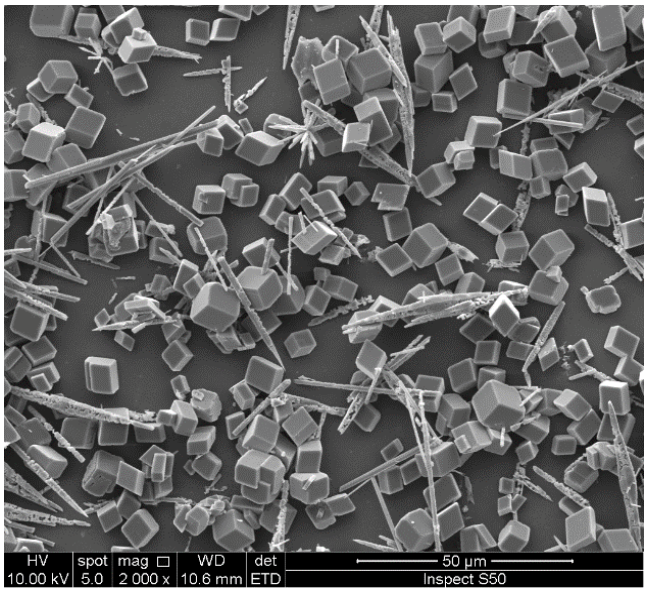

Fig. 5. SEM image of $CaCO_3$ in blank water.

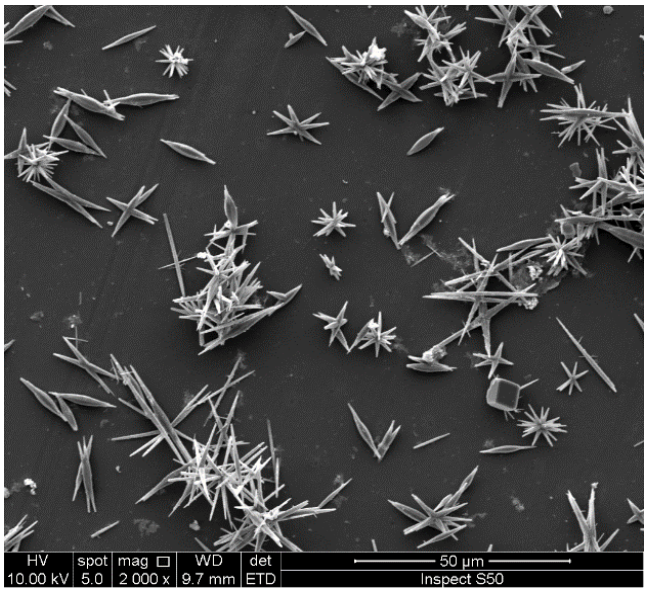

Fig. 6. SEM image of $CaCO_3$ with the electrostatic field.

3.2.2. XRD analysis of $CaCO_3$

The XRD pattern of $CaCO_3$ scale from the blank water sample is shown in Fig. 9(a). The diffraction peaks at approximately 23°, 29°, and 39° were characteristic peaks of calcite.

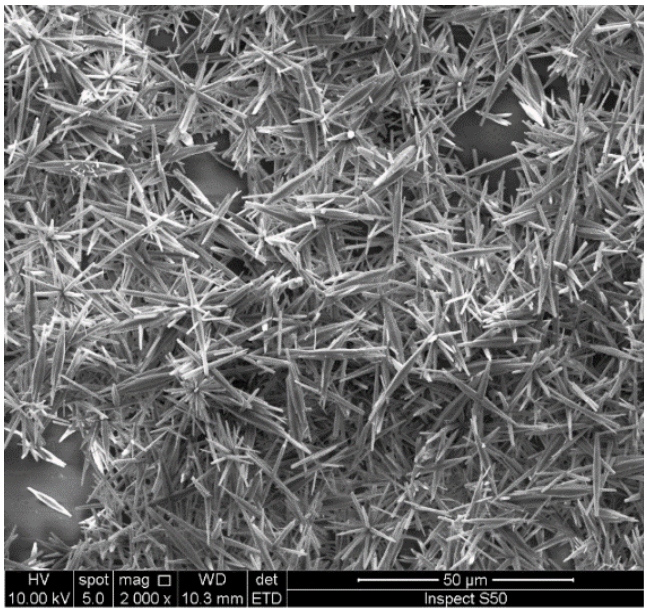

Fig. 7. SEM image of $CaCO_3$ with the copolymer.

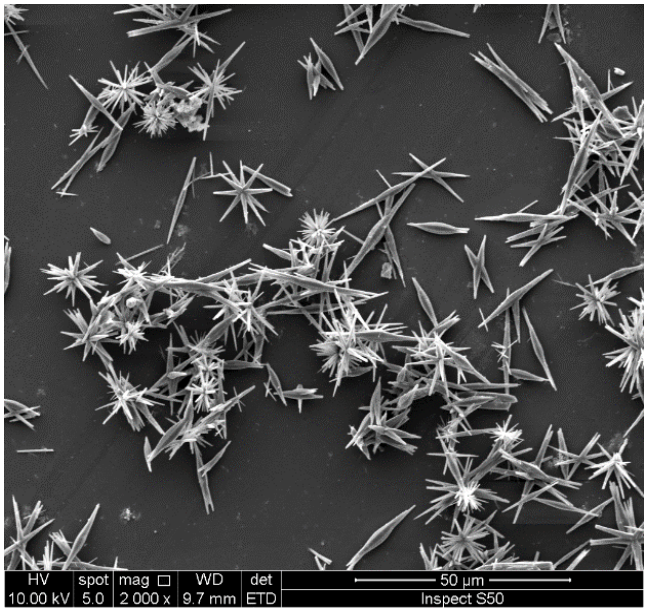

Fig. 8. SEM image of $CaCO_3$ with the copolymer and electrostatic field.

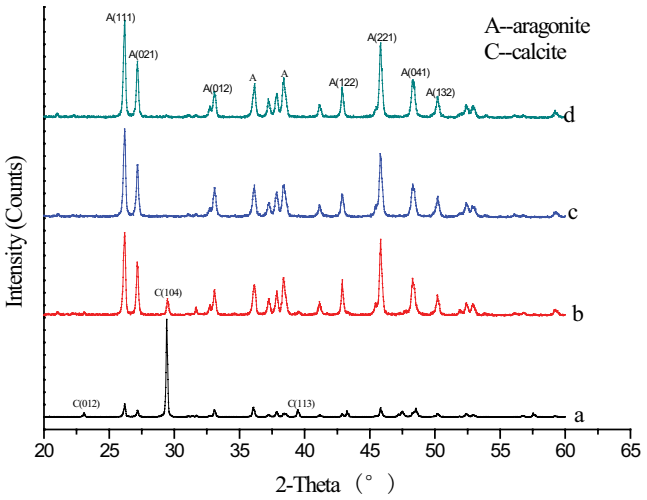

Fig. 9. XRD patterns of $CaCO_3$ sample formations under different conditions. (a) The XRD pattern of $CaCO_3$ in blank water. (b) The XRD pattern of $CaCO_3$ in water treated with an electrostatic field. (c) The XRD pattern of $CaCO_3$ in water treated with ESA/IA/AMPS copolymer. (d) The XRD pattern of $CaCO_3$ in water treated with an electrostatic field and ESA/IA/AMPS copolymer.

The diffraction peaks at approximately 26°, 27°, 33°, 36°, 45°, 48°, and 50° were the characteristic peaks of aragonite. It calculated that the content of calcite was 83.8% and the aragonite was 16.2%.

The XRD pattern of $CaCO_3$ from the water sample treated with an electrostatic field is shown in Fig. 9(b). Compared with the pattern in (a), the calcite diffraction peak at 29.480° was weaker, and the aragonite peaks at approximately 26°, 27°, 33°, 36°, 38°, 42°, 45°, 48°, and 50° were larger in pattern (b). It calculated that the content of calcite was 4.5%, and the content of aragonite was 95.5%. The electrostatic field facilitated the formation of aragonite. When water samples are treated with an electrostatic field, water molecules are activated, and the dipole moment and polarity increase [17–19]. Additionally, the hydration of positive and negative ions increases, therefore, Ca^{2+} and CO_3^{2-} are less likely to knock against each other and form $CaCO_3$ crystal. Meanwhile, electrostatic attraction between the Ca^{2+} and CO_3^{2-} ions changes. This affects the nucleation rate of the crystal, altering the crystal structure. Moreover, the field energy changes the crystal face free energy of the crystal and affects the growth of the crystal nucleus.

As shown in Figs. 9(c) and (d), the diffraction peak of calcite disappeared, and the remaining peaks were characteristic of aragonite. This suggests that the $CaCO_3$ crystal was aragonite when the water sample was treated with the copolymer or the copolymer and electrostatic field together. The results were in good agreement with SEM images. When an electrostatic field and copolymer were applied in combination, the activated water and copolymer molecules bonded to produce more dispersed $CaCO_3$ particles.

4. Conclusions

A synergistic scale inhibition effect was observed when an electrostatic field and ESA/IA/AMPS copolymers were used in water treatment. The concentration of the copolymer and the applied electrostatic voltage affected the synergism. When the electrostatic voltage was 5 kV and the copolymer concentration was 1.0 mg/L, the synergistic scale inhibition rate was 95.85%, which increased by 12.94% when compared with that used the copolymer alone. This study provides a feasible water treatment method that reduces the dosage of chemical inhibitors and environmental pollution.

The SEM and XRD results show that the use of the electrostatic field favored the formation of aragonite $CaCO_3$. The synergistic effect between the electrostatic field and the copolymer resulted in looser scale that did not easily adhere to the heat exchanger surface. This was due to that $CaCO_3$ crystal formation was hindered by the electrostatic field. Additionally, the $CaCO_3$ microcrystals adsorbed to the copolymer and the normal growth of $CaCO_3$ crystals is altered.

Acknowledgment

This work was financially supported by the National Natural Science Foundation of China (21376062) and Hebei Province Applied Basic Research Program-Key Basic Research Project (18964005D).

References

[1] Q. Chen, J. Ye, J. Xiong, Introduction of 2016 Presidential Green Chemistry Challenge Awards, Chem. Ind. Eng. Prog., 35 (2016) 3002–3003.
[2] P.T. Anastas, M.M. Kirchhoff, Origins, current status and future challenges of green chemistry, Acc. Chem. Res., 35 (2002) 686–694.
[3] G.S. Fanourgakis, An extension of Wolf's method for the treatment of electrostatic interactions: application to liquid water and aqueous solutions, J. Phys. Chem. B, 119 (2015) 1974–1985.
[4] B. Wiedenfeld, Effects of irrigation water salinity and electrostatic water treatment for sugarcane production, Agric. Water Manage., 95 (2008) 85–88.
[5] W. Liu, F. Hui, J. Lédion, X. Wu, Inhibition of scaling of water by the electrostatic treatment, Water Resour. Manage., 23 (2009) 1291–1300.
[6] M. Sun, Z. Liu, W. Wang, H. Wu, Study on applying high voltage electrostatic to treat microorganisms in cooling water system of power plants, Energy Conserv. Technol., 28 (2010) 206–208.
[7] X. Wu, T. Gao, Low voltage electrostatic water treatment for scale inhibition, J. Tongji Univ.: Nat. Sci. Ed., 24 (1996) 411–416.
[8] S.H. Lee, A Study of Physical Water Treatment Technology to Mitigate the Mineral Fouling in a Heat Exchanger, Drexel University, Michigan, USA, 2002.
[9] C.A. Bennett, An Investigation into Electrostatic Water Treatment Systems, Lehigh University, Bethlehem, 2002.
[10] K. Uemura, S. Isobe, Developing a new apparatus for inactivating *Escherichia coli* in sailing water with high electric field AC, J. Food Eng., 53 (2000) 203–207.
[11] D. Liu, W. Dong, F. Li, H. Franck, J. Lédion, Comparative performance of polyepoxysuccinic acid and polyaspartic acid on scaling inhibition by static and rapid controlled precipitation methods, Desalination, 304 (2012) 1–10.
[12] L. Zhang, Z. Zhu, Chromium extraction from sewage sludge using polyepoxysuccinic acid, Pedosphere, 22 (2012) 131–136.
[13] L. Zhang, Z. Zhu, Y. Qiu, R. Zhang, J. Zhao. Determination of the dissociation constants of polyepoxysuccinic acid, Environ. Sci. Eng. China, 2 (2008) 505–508.

[14] T. Gu, P. Su, X. Liu, J. Zou, X. Zhang, Y. Hu, A composite inhibitor used in oilfield: MA-AMPS and imidazoline, J. Pet. Sci. Eng., 102 (2013) 41–46.
[15] A. Zhang, G. Zhang, H. Wei, L. Liu, Preparation and performance of a new sulfonate copolymer scale inhibitor, Chem. Ind. Eng. Prog., 30 (2011) 1858–1861.
[16] Z. Liu, Z. Liu, X. Li, X. Wang, Synthesis characterization and properties of the ESA/AMPS copolymer, Sci. Technol. Eng., 13 (2013) 2124–2127+2137.
[17] M. Gao, H. Li, L. Zhang, X. Bai, Z. Liu, Study on synthesis, scale inhibition performance and mechanism of ESA/IA/AMPS copolymer, Fine Chem., 34 (2017) 42–47.
[18] H. Li, Z. Liu, Y. Gao, X. Li, L. Zhang, Influence of high-voltage electrostatic field on the scale inhibition performance environmentally friendly scale inhibition agent and the crystal forms of scale, Technol. Water Treat., 39 (2013) 24–27.
[19] H. Li, Z. Liu, Y. Gao, L. Zhang, X. Li, Influence of electrostatic water treatment on crystallization behavior of $CaCO_3$ and synergistic scale inhibition with a green scale inhibitor, J. Chem. Ind. Eng., 64 (2013) 1736–1742.